Physics 450

Particle Physics at the Large Hadron Collider

outline of the course:

- general features of hadron collisions at high energy
- the parton model
- computation of $O(\alpha_s)$ QCD corrections
- jets, jet observables, and parton showers
- computation of QCD multi-jet cross sections
- the top quark and the Higgs boson at the LHC.

Hadron-Hadron Collisions at High Energy

We are now all waiting expectantly for the start of physics at the Large Hadron Collider. This accelerator will produce proton-proton collisions at a center of mass energy of 14 TeV. It will have the capability of testing essentially all proposed models of new physics beyond the Standard Model. It will be able to produce new particles with masses of 2 TeV and beyond.

However, experimentation at the LHC will require a great deal of understanding of the Standard Model and, especially of QCD. The cross sections for the pair production of new particles are of the order of 1-10 pb. These reactions will compete for attention with Standard Model reactions with much higher cross sections:

$t\bar{t}$ production	~ 1 nb
W, Z production	$\sim$ 300, 100 nb
2-jet w. $p_T > 100$	$\sim 2\,\mu$b
$b\bar{b}$	~ 1 mb
$\sigma_{tot.}$	$\sim$ 100 mb

so that, finally

$$\sigma_{tot}(pp) \sim 10^{10} \cdot \quad 10\,pb \quad !$$

The hierarchy of reactions is shown in the Fig. p.2.
To understand how to observe new physics, we need to understand all of these reactions in great detail. We need to understand what their cross sections are, but also, what the events look like and how we can use detailed measurements of the final states to distinguish them from new particles. We need to understand what more complex events these reactions can generate at higher orders in QCD.

In this course, I will make a detailed introduction to QCD at high energy colliders. I will discuss some topics that are taken from a standard Quantum Field Theory course and others that lie at the next level. We will not quite get to the current state of art, but I hope that this course leaves you prepared to go there.

Most of the course will be devoted to large momentum transfer reactions in QCD. However, we should begin with a discussion of the total cross section in $p\bar{p}$ scattering and the typical events that make up this

cross section - that will be the subject of this lecture.

All hadron - hadron total cross sections have the same systematics. At low energy, they are dominated by individual hadronic resonances. This is shown for the πp cross section in Figs. 9.3 (taken from the textbook of Gasiorowicz). At higher energy, the resonances begin to overlap and become broader. Eventually, they wash out and give a total cross section of a constant value:

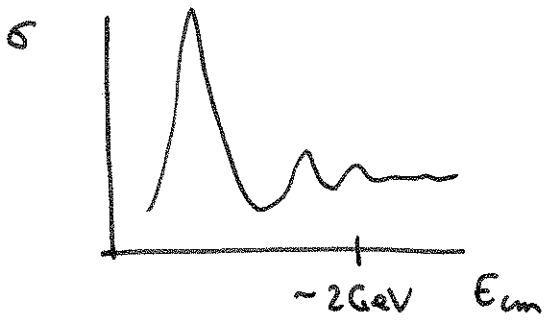

You might think of this constant as the geometrical cross section of the discs that represent the Lorentz-contracted quark-gluon bound states at high energy:

Indeed, roughly $\sigma_{pp} \sim \frac{3}{2}\sigma_{\pi p}$. Even γp and $\gamma\gamma$ cross sections have this "black disk" behavior,

with $\sigma_{\gamma p} \sim \alpha \sigma_{\pi p}$ $\sigma_{\gamma\gamma} \sim \alpha^2 \sigma_{\pi p}$. You might imagine that the photon becomes a virtual ρ meson, which is then a hadron and has a black disc structure.

Figs p. 4 show these cross sections and their extrapolation to very high energy. For $p\bar{p}$ we have cross section measurements at the Tevatron (1.8 TeV), and for pp we have very high E_{cm} measurements from cosmic rays. The data show a slow increase, which can be fit by

$$\sigma_{tot} \sim A \log^2 s$$

(more detail in Fig. p. 5)

This can be explained by the process of the creation of virtual pions (and other hadrons) at the edge of the black disc:

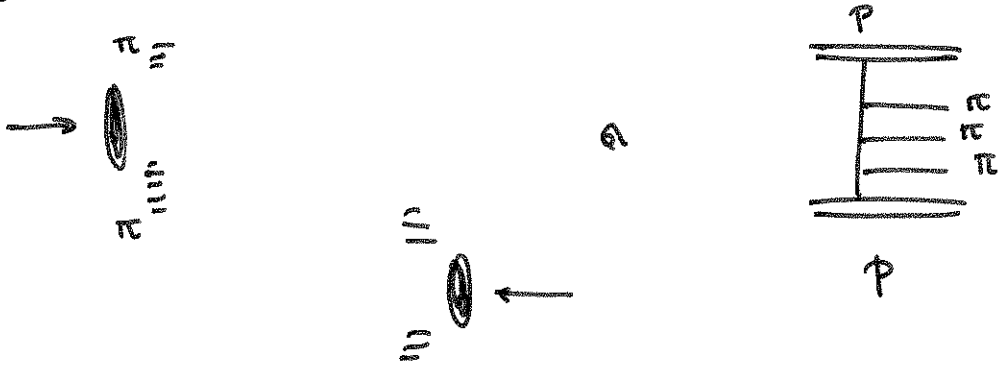

Froissart analyzed this process using the partial wave expansion for pp scattering and proved that, in any theory in which the lightest particle has mass m_π, unitarity implies the bound:

$$\sigma_{tot} < \frac{2\pi}{m_\pi^2} \log^2 \frac{s}{m_\pi^2}$$

This is called the Froissart bound. The value of the bound is about 4000 mb at $\sqrt{s} = 1$ TeV — well above the measured values — but the bound limits the rate of growth of σ_{tot}.

A typical pp event at high energy contains many particles. The growth of the charged particle multiplicity is shown in fig. p. 6. The rise is fit by a function of the form

$$n_{ch} \sim \exp\left[A\sqrt{\log s}\right]$$

Typically, $n_{ch} \sim 100$ at LHC energies. (It will be important to measure this in the early running at the LHC.)

You might be tempted to conclude from this that elastic scatt, $pp \to pp$, is completely unimportant at LHC energies. However, a little thought indicates that there must be a sizable elastic component. The optical theorem related the forward elastic scatt cross section to the total cross section. So, at least in the very forward direction, the elastic process must be there. The interference of the forward elastic cross section with the incoming wave creates the shadow behind the black disc.

Let's analyze this. The optical theorem

implies: $\mathrm{Im}\, \mathcal{M}(\theta=0) = 2 E_{cm} p_{cm} \sigma_{tot}$

$\cong s \cdot \sigma_{tot}$ for $s \gg m_p^2$

The statement that $\mathcal{M}(\theta=0)$ is purely canceling the incoming wave implies that $\mathcal{M}$ is pure imaginary. It is actually possible to measure the phase of $\mathcal{M}(0)$ at the energies where σ_{tot} is approximately constant (for example, at the ISR ($E_{cm} = 53$ GeV), by measuring the interference of the strong-interaction and Coulomb scattering amplitudes). The results are shown in Fig. p. 7, and indeed

$$\left| \frac{\mathrm{Re}\, \mathcal{M}}{\mathrm{Im}\, \mathcal{M}} \right| < 0.15.$$

If we ignore $\mathrm{Re}\, \mathcal{M}$, the above relation implies

$$\left. \frac{d\sigma}{d\cos\theta} \right|_{\theta=0} = \frac{1}{2s} \frac{1}{16\pi} |\mathcal{M}(0)|^2$$

$$= \frac{1}{32\pi} s \, \sigma_{tot}^2$$

We might also expect that $\frac{d\sigma}{d\cos\theta}$ falls off rapidly with $\cos\theta$ or with $t = -2p^2(1-\cos\theta)$. Diffraction from a disk of fixed size predicts that the width of the cross section is

$$\Delta\theta \sim 1/E_{cm}$$

motivating the parametrization:

$$\frac{d\sigma}{dt} \sim e^{bt} \sim \exp\left[-\tfrac{1}{2} bs(1-\cos\theta_{cm})\right]$$

which is a good representation of the data (Fig. - p. 8). At $E_{lab} = 10$ GeV, $b = 10\ (\text{GeV})^{-2}$. As the disc expands, b should grow like $\log s$. Integrating this formula using the value of $\frac{d\sigma}{dt}(t=0)$ on p. 8)

$$\frac{d\sigma}{dt} = \frac{1}{16\pi}\sigma_{tot}^2\, e^{bt}$$

$$\sigma_{elastic} = \frac{1}{16\pi b}\sigma_{tot}^2 \sim (0.2-0.3)\,\sigma_{tot}.$$

This is a large component of σ_{tot}. Then, at LHC energies.

$$\sigma_{inelastic} \sim 70\text{-}80\ \text{mb}$$

In addition to elastic scattering

there is another class of low-multiplicity reactions in which one proton is excited to a low-mass resonance

This is called "diffractive dissociation".

It is not so easy to observe these diffractive reactions at the LHC. As we'll discuss next time, the LHC detectors are optimized by large angle scattering. Very forward tracks go down the beam pipe. An experiment called TOTEM will put detectors in the accelerator beam pipe near the CMS experiment, including detectors encased in ceramic ("Roman pots") at 147, 180, & 220 m. upstream, to detect forward-scattered protons. (see Fig. p.9)

One final property of the diffractive component is the Pomeranchuk theorem, the equality of particle and antiparticle cross sections:

$$\sigma_{tot}(AB) - \sigma_{tot}(A\bar{B}) \to 0 \quad \text{as} \quad s \to \infty$$

This result is clearly obeyed by the data in Fig. p. 4, 5.

Here is a simplified proof of the theorem, assuming $\sigma_{tot.} \to$ const as $s \to \infty$:

Consider $\mathcal{M}(s, t=0)$, the elastic AB scattering amplitude, as an analytic function of s. The singularities of this function correspond to physical intermediate states. There are two branch cut singularities in the complex s plane:

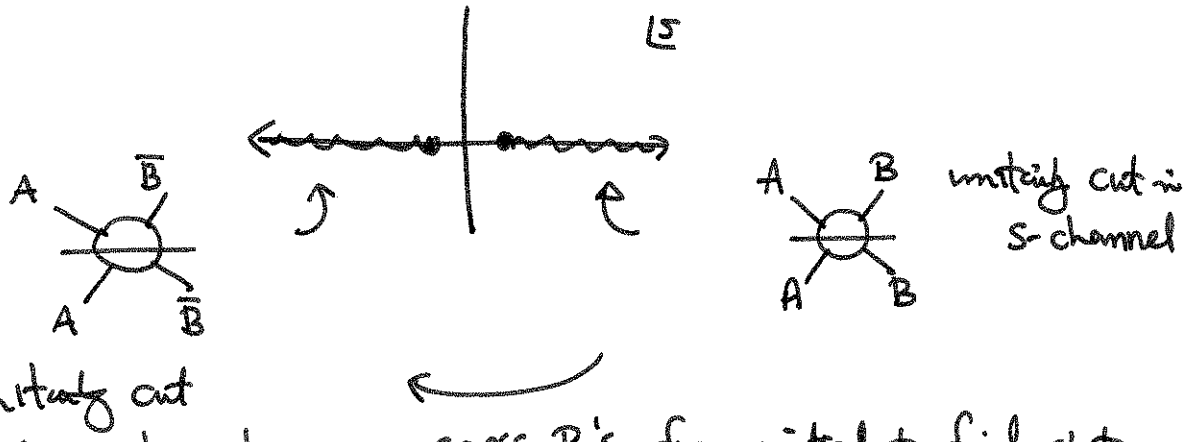

$s+t+u = O(m_p^2)$ so $u \cong -s$ at high energy

on the right-hand cut $\quad \mathrm{Im}\,\mathcal{M} = s\,\sigma_{tot}(AB)$

on the left-hand cut $\quad \mathrm{Im}\,\mathcal{M} = u\,\sigma_{tot}(A\bar{B})$

Now we need to repeat $\mathcal{M}$ by an analytic function that joins up correctly at $s \to \infty$. If we write

$$\mathcal{M} \to \pm i\, C_1\, s \qquad \text{above / below the cut}$$

this gives $\quad C_1 = \sigma_{tot}(AB) = \sigma_{tot}(A\bar{B})$

We could also have a component

$$\mathcal{M} \to C_2 \frac{s}{\pi} \log s$$

$$\sigma_{tot.}(AB) = C_1 + C_2 \qquad \sigma_{tot}(A\bar{B}) = C_1 - C_2$$

However, $C_2 \neq 0$ implies $\mathrm{Re}\,\mathcal{M}/\mathrm{Im}\,\mathcal{M} \sim \log s$,

so if $\mathrm{Re}\,\mathcal{M}/\mathrm{Im}\,\mathcal{M}$ is bounded, $C_2 = 0$ and $\sigma(AB) = \sigma(A\bar{B})$

in the limit of large s.

By adding appropriate factors of $\log s$, this argument can be made to work for a rising cross section $\sigma(AB) \sim \log^2 s$.

Now let's discuss the high-multiplicity processes that dominate the total cross section. A first picture of these events comes from the model of the proton as a bag of weakly interacting quarks and gluons. A proton-proton collision shatters the bag, jolting the constituents

This results in a hot gas of quarks and gluons, all at relatively low values of p_T. If the gas is locally at a fixed temperature, we would expect an exponential fall-off

$$e^{-p_T/T}$$

and this is not a bad fit to the data on the p_T distribution, shown in Figs. p.10 for fixed-target pp scattering. The great majority of particles have $p_T < 1$ GeV

The final state does have quarks and gluons moving at large momentum in the longitudinal direction, parallel to the original direction of the proton beams. Essentially, the proton constituents ("partons") share the momentum of the original proton. Each

parton-parton collision has a different center of mass frame, longitudinally boosted with respect to the others. To describe this situation, it is useful to choose a new coordinate system that transforms simply under longitudinal boosts.

Begin with a 4-vector with $p^3 = 0$

$$p^\mu = (E, \vec{p}_T, p^3) = (E_T, \vec{p}_T, 0)$$

$E_T = (m^2 + p_T^2)^{\frac{1}{2}}$ is the "transverse energy"

Now boost in the $\hat{3}$ direction

$$p^\mu \rightarrow (E_T \cosh y, \vec{p}_T, E_T \sinh y)$$

where $\cosh y = \gamma$ $\sinh y = \beta\gamma$ $\cosh^2 y - \sinh^2 y = \gamma^2(1-\beta^2) = 1$

y is called the rapidity. Under a further boost along the $\hat{3}$ axis

$$p^0 \rightarrow \gamma' E_T (\cosh y + \beta' \sinh y)$$
$$p^3 \rightarrow \gamma' E_T (\beta' \cosh y + \sinh y)$$

so if we write $\gamma' = \cosh \Delta y$ $\beta'\gamma' = \sinh \Delta y$

$$p^0 \rightarrow E_T \cosh(y + \Delta y)$$
$$p^3 \rightarrow E_T \sinh(y + \Delta y)$$

A longitudinal boost is a translation of y. If we use the variables

(y, ϕ, p_T) instead of (θ, ϕ, p)

to describe a final state, a boosted final state will look identical except for a shift in y. This will be very convenient.

Often, we have not identified the specific particles responsible for tracks or measured energy deposition, so we do not know the masses. However, when $p_T \gg m$, the mass is irrelevant. So we often use the formulae above assuming $m=0$. Then

$$p^\mu \cong (p_T \cosh\eta, \vec{p}_T, p_T \sinh\eta) \qquad E_T = p_T$$

η is called pseudo-rapidity. η is directly related to the polar angle θ:

$$\cos\theta = \frac{p_T \sinh\eta}{p_T \cosh\eta} = \tanh\eta$$

The inverse of this relation is

$$\eta = \frac{1}{2} \log \frac{(1+\cos\theta)}{(1-\cos\theta)}$$

In collider physics, we will usually use η rather than θ to express angles. However, be warned: A small excursion in η easily takes one to very forward angles

$$\eta = 5 \text{ corresponds to } \theta = 0.77^\circ = 0.013 \text{ rad.}$$

It is hard to measure tracks closer to the beam than that.

Figs p. 11 shows an axial view of a typical $p\bar{p}$ event observed by the CDF detector at the Fermilab Tevatron.

The event is extremely complex, with 30-40 tracks. An alternative view of this event is shown in Figs. p.12. In this figure, we use the (η, ϕ) coordinate system and plot p_T as a height above the (η, ϕ) plane. This plot, called the "Lego plot", is a very useful way to view collider events. Figs. p.13, 14 show another example.

A first picture of particle production in hadron-hadron collisions is given by the "Feynman-Wilson gas" model. The collision, as described on p.12, leads to a multiplicity distribution

$$n(\vec{p}) \sim (\text{uniform in } y, \phi) \cdot e^{-c|p_T|}$$

$c \sim \frac{1}{300 \text{ MeV}}$.

Typical "minimum bias" events have the form

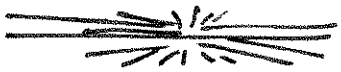

in a usual coordinate system but look simple

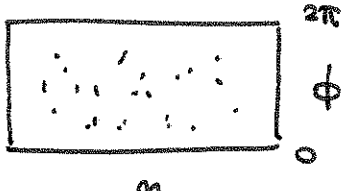

on the lego plot. It is important to remember that this distribution of low p_T particles goes out to high

values of η, while detectors can see $|\eta| < 4$-5 only.

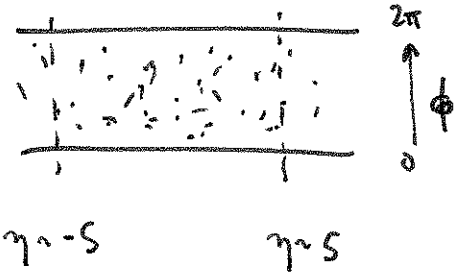

Particles nearby in η ($\Delta\eta \sim 1$) tend to be correlated in momentum and flavor.

However, this is not the whole story. Figs. p. 15 shows the evolution of the transverse momentum distribution of single particles from fixed-target energies to the Tevatron (1.8 TeV). At about 10^{-4} of the total rate, we see a clear deviation from the exponential fall off. Figs p 16 shows a clearer view of the Tevatron results.

It is quite remarkable to see what the events look like that contain these high-p_T particles. Figs. 17, 18 shows an example. The axial view in the tracking chamber is superficially similar to those in the "minimum bias" cases. However, the lego plot looks very different. We see two high towers, approximately back to back in ϕ, apparently superposed on a uniform background of low-p_T particles from a Feynman-Wilson gas

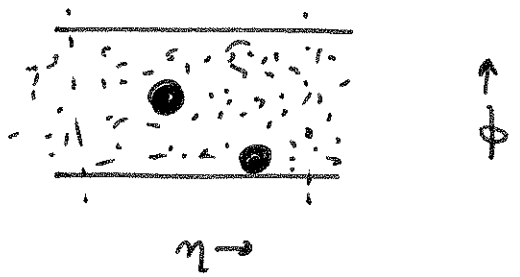

These towers come from collimated bunches of high-p_T particles. These are called "jets". I will interpret jet events as events with hard scattering between individual partons. Later in the course, I will explain how to predict the cross sections and angular distributions for these events.

Jet events run over the full dynamic range available at a hadron-hadron collider. Figs. p. 19, 20 shows an impressive event containing a 90 GeV-p_T jet. At the other extreme, Figs. p. 14, a "minimum bias" event, contains a small jet of $p_T \sim 7$ GeV at $\eta \sim -1$ $\phi \sim 20°$. It is an interesting question to what extent minimum bias events contain jets. It is likely that, at LHC energies, almost all events will contain visible jets, often more than one pair. This needs to be investigated with early data.

Still more complex events are possible. Figs. p. 21 show a CDF event with four jets. Such an event might indicate the production of a new heavy particle, but,

more likely, it is the result of parton-parton scattering with extra gluon radiation. We need to know how to predict the cross section for QCD events of this type. This will be an important topic in the course.